

The Role of Quantum Confinement in p-Type Doped Indium Phosphide Nanowires

M. M. G. Alemany,^{*,†} Xiangyang Huang,[‡] Murilo L. Tiago,[§] L. J. Gallego,[†] and James R. Chelikowsky^{§,||}

Departamento de Física de la Materia Condensada, Facultad de Física, Universidad de Santiago de Compostela, E-15782 Santiago de Compostela, Spain, Department of Chemical Engineering and Materials Science, University of Minnesota, Minneapolis, Minnesota 55455, Center for Computational Materials, Institute for Computational Engineering and Sciences, University of Texas, Austin, Texas 78712, and Departments of Physics and Chemical Engineering, University of Texas, Austin, Texas 78712

Received February 12, 2007; Revised Manuscript Received May 12, 2007

ABSTRACT

The impurity state responsible for current flow in zinc-doped indium phosphide nanowires is characterized through first-principles calculations based on a real-space implementation of density functional theory and pseudopotentials. The binding energy of the acceptor state is predicted to range from the value of the acceptor state in the bulk up to values of ~ 0.2 eV in the thinner nanowires as a result of the two-dimensional quantum confinement. The location of the impurity atom within the nanomaterial is not found to play a prominent role in determining the characteristic properties of the state. Our results show that, in thin nanowires, quantum confinement can move the defect level deep into the energy gap.

The historical rates of improvement in productivity experienced by the semiconductor industry during the last decades are based on a continued miniaturization of silicon-based devices. However, existing materials and technologies are approaching their physical limits, which will soon prevent the industry from reaching similar rates of improvement.¹ Finding new materials and technologies adequate for the fabrication of highly integrated devices within the nanometer regime would potentially overcome such limitations. Among the materials probed for this application, semiconductor nanowires (NWs) are of special interest. One-dimensional materials like NWs are nanostructured materials that can transport efficiently electrical carriers and optical excitations. NWs with controlled electrical and optical properties can be synthesized from a wide variety of semiconductor species. They have also been used as basis for working devices.² As such, NWs are considered ideal building blocks for highly integrated nanoscale electronics and optoelectronics.

Indium phosphide NWs (InP-NWs) are among the NWs for which very promising advances have been made. Energy band gaps and photoluminescence images and spectra of InP-NWs have been determined experimentally.^{3,4} Doped InP-NWs growth as p-type NWs are known to function as light-emitting diodes and field electric transistors when assembled with n-type NWs.^{2,5} However, little is known about fundamental issues behind these findings. For example, the nature of the electronic states that allow transport in the doped InP-NWs are yet to be characterized. Are these states, often obtained by energy band engineering, spatially localized or extended states? Also, how does quantum confinement affect the electronic properties? Answering these questions is not only important from a fundamental point of view. It could also be relevant for designing future devices and applications based on InP-NWs, as well as to improve current designs. Here we address these issues by performing first-principles calculations on p-type doped InP-NWs. In particular, we find that the presence of free carriers in the NW is limited by the effect of quantum confinement on the binding energy of the acceptor impurity state.

We have studied p-type doped InP-NWs obtained through the introduction of Zn impurities in the host NW, following experimental techniques for p-type doping.⁵ Our calculations are based on pseudopotentials constructed within density

* Corresponding author. E-mail: alemany@usc.es.

[†] Departamento de Física de la Materia Condensada, Facultad de Física, Universidad de Santiago de Compostela.

[‡] Department of Chemical Engineering and Materials Science, University of Minnesota.

[§] Center for Computational Materials, Institute for Computational Engineering and Sciences, University of Texas.

^{||} Departments of Physics and Chemical Engineering, University of Texas.

functional theory as implemented in the PARSEC code.⁶ In this implementation, the Kohn–Sham equations are solved self-consistently on a rectangular three-dimensional real-space grid within a supercell geometry.⁷ Only one parameter, the grid spacing, is necessary to control numerical convergence. The core electrons are represented by norm-conserving *ab initio* pseudopotentials.⁸ The local density approximation (LDA) is used for the exchange and correlation potential.⁹ Our approach is specially devised for the accurate study of large, complex systems with numerous degrees of freedom, and it is specifically targeted for the nanoscale.^{6,7}

Cylindrical models of InP-NWs are constructed from the bulk oriented along the [111] direction of the zinc-blende structure. In and P dangling bonds at the surface of the NW are passivated using fictitious, hydrogen-like atoms with fractional charge.¹⁰ The passivation is performed in such a way that no In or P atom is bonded to more than two fictitious atoms. These model NWs are chosen to mimic experimental conditions. High-quality InP-NWs with nearly monodisperse diameter and crystalline core with axis direction determined as [111] are grown from nanoparticle catalysts.^{3,11} Surface states in experimentally obtained InP-NWs are made electronically inert by an amorphous coating layer.^{5,11}

One axis of the rectangular supercell (*z*-axis) is aligned parallel to the growth direction of the NWs. The length of the supercell in this dimension is chosen to keep the periodicity of the NWs. The primitive cell includes three InP layers along [111], having a size $L_z = \sqrt{3}a$, with *a* being the bulk lattice constant.¹² The size of the supercell in the perpendicular directions is large enough to suppress the interactions between the NW and its periodic images. A spacing of 0.52 au (1 au = 0.529 Å) is used for constructing the real-space grid, and the single Γ point is employed in sampling the Brillouin zone. InP-NWs are known to retain the direct-band character of the bulk, in according with previous theoretical results.¹³ The ionic positions of the atoms are not allowed to relax. Owing to weak interatomic forces obtained from this analysis, the effect of structural relaxation on the NW electronic structure is expected to be small. This is in keeping with a recent first-principles study on germanium NWs.¹⁴

The computed enhancement of the energy gap of the NWs with respect to the bulk energy gap is compared with experiment in Figure 1. Values corresponding to the relaxed NWs are estimated to be within 0.01 eV from those reported in Figure 1. Our results are consistent with previous first-principles results performed within the LDA.¹⁵ We observe a significant widening of the energy gap with decreasing size of the NWs, indicating stronger quantum confinement in the NWs. Our results match experiment, although a careful interpretation of the theoretical results should be carried out. It is well-known that approaches based on the LDA underestimate the experimental energy gaps. For the sizes of the NWs where both theory and experiment overlap (see Figure 1), the self-energy correction to the Kohn–Sham band

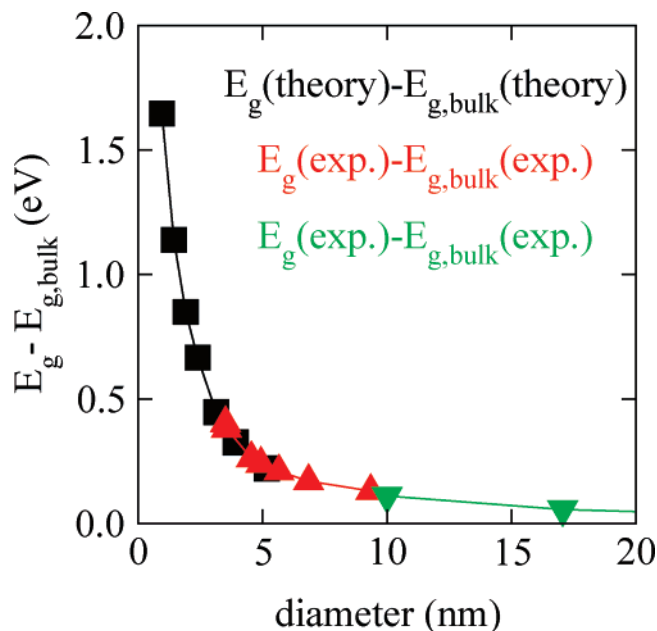


Figure 1. Energy gap of InP nanowires as obtained from theory (black squares) and experiment (red triangles, ref 3; green triangles, ref 4). The energy gap of the bulk is chosen as reference. The data from theory correspond to nanowires with diameters 0.96, 1.43, 1.91, 2.39, 3.13, 3.92, and 5.17 nm.

gap¹⁶ does not depend on the size of the NWs. The self-energy correction taken from the bulk is ~ 0.4 eV, i.e., the theoretical bulk gap is 1.01 eV, whereas experiment is 1.42 eV. This situation will likely change for smaller NWs. Recent computations on small silicon¹⁷ and germanium¹⁴ NWs have shown that the self-energy correction increases monotonically with decreasing diameter of the NWs. This will give a variation of the energy gap of the NWs with their size more pronounced than that shown in Figure 1. Energy levels that are valence-band derived are expected to be moderately affected by band gap corrections as discussed elsewhere.¹⁶ As such, the LDA formalism is expected to be capable of properly describing acceptor impurity states.

We are interested in determining both the character and binding energies of the acceptor impurity states introduced in the NW by a Zn impurity. The binding energy E_b of a given impurity state is calculated as the position of the impurity level with respect to the valence band maximum (VBM) of the host material. The calculation of the latter level often requires estimating the potential energy shift introduced by the impurity. For a supercell geometry, the VBM is used as a reference level, i.e., our calculation of E_b is obtained referenced to the VBM calculated for the impurity-free supercell.¹⁸ A common practice is to align the screened potentials obtained for the impurity-containing and impurity-free supercells in a region far from the impurity.¹⁸ In our work, the alignment is performed after evaluating and averaging the potentials in the interstitial region of the NWs farthest from the impurity.

For Zn to be an electrically active acceptor in InP, it must reside substitutionally in a cation site: Zn_{In} . The acceptor

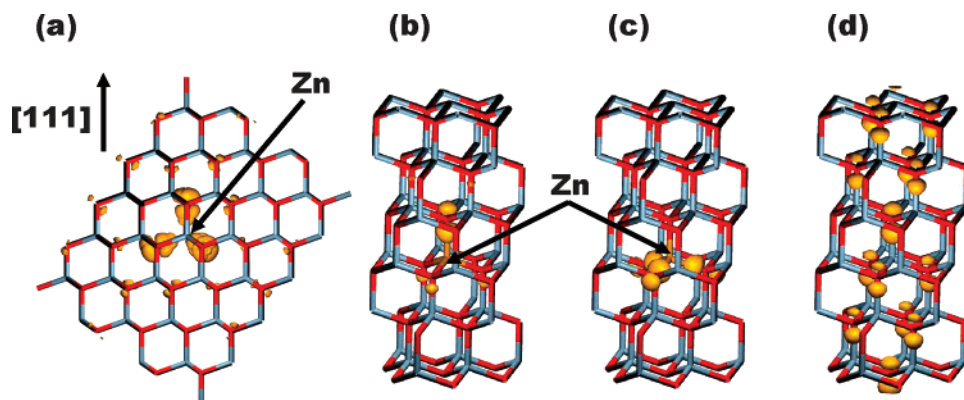


Figure 2. Charge density associated to one of the impurity states introduced in bulk InP and InP nanowires (InP-NWs) by Zn doping as obtained from our real-space first-principles approach (panels a–c): (a) Triply degenerate acceptor state introduced in bulk InP. (b) Singly degenerate acceptor state introduced in InP-NWs. (c) Doubly degenerate state introduced in InP-NWs. (d) Charge density associated to the state determining the valence band maximum in InP-NWs. The charge density is plotted at the 25% of its maximum value for all (a–d). Gray (red) symbols stand for In(P) atoms. (Hydrogen-like atoms used to saturate dangling bonds in the NWs are not shown.) The wire models of InP-NWs in (b–d) correspond to the NW with diameter 0.96 nm.

state introduced in bulk InP by Zn_{In} is measured to be very shallow with a binding energy in the range of 0.033–0.055 eV.¹⁹ We have identified this state as a triply degenerate state with t_2 symmetry. The state possesses anion p character, as depicted in Figure 2a. We note that this state is not highly localized, despite being mostly concentrated at the Zn–P bonds formed by the impurity atom and its nearest neighbors. Significant contribution at other P sites exist. We can extrapolate to the bulk limit by means of an exponential fit.²⁰ Using cubic supercells with sizes ranging from 64 to 2744 atoms gives a binding energy for this state of 0.034 eV.

The highly anisotropic nature of the nanowire breaks the tetrahedral symmetry of the impurity potential and splits the triply degenerate impurity state into singly and doubly degenerate states. The singly degenerate state corresponds to the charge density of the bulk t_2 impurity state mainly distributed along the axial direction of the NWs, i.e., along the Zn–P bond aligned in the $[111] \equiv \hat{z}$ direction (Figure 2b). The doubly degenerate state accounts for the rest of the charge density of the state, i.e., the charge density mostly contained in the radial dimension of the NWs (Figure 2c). Owing to the much stronger confinement it experiences, this latter state has an energy level lower than the singly degenerate state, i.e., the *acceptor state*. Both the acceptor level and the level corresponding to the VBM in the pure NW (see Figure 2d) share the same symmetry character, characteristic of anion p_z states. As a consequence, the acceptor state exhibits some delocalization along the growth direction of the NW.

The proper location of the impurity levels in the host band structure requires an estimate of impurity–impurity interactions. This can be done in a natural way within a supercell approach, where one Zn_{In} impurity is included in each supercell. In the simulated NWs, Zn_{In} impurities are separated by a distance L_z along the growth direction of the NWs, as illustrated in the inset of Figure 3. The effects derived from impurity–impurity interactions can be evaluated by considering supercells with different L_z sizes. The chosen sizes are consistent with the structure of the NWs, namely:

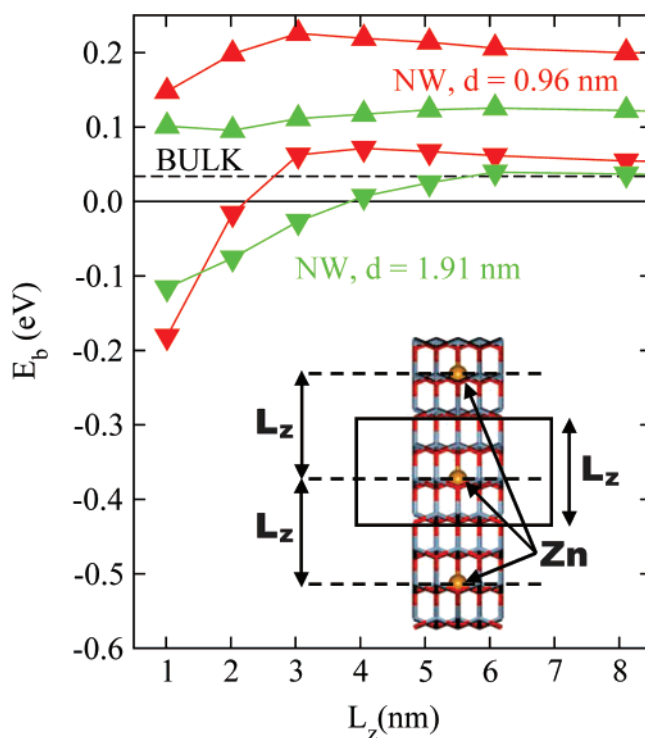


Figure 3. Binding energy of singly (up triangles) and doubly (down triangles) degenerate impurity states introduced in InP nanowires obtained for different sizes L_z of the supercells. Data correspond to nanowires (NWs) with different diameters d . The binding energy of the acceptor state introduced in bulk InP computed in the isolated impurity limit is also shown (dashed line). The inset represents a Zn-doped NW as studied within the supercell approach.

$L_z = n \times \sqrt{3}a$, with n representing the number of primitive cells contained in the supercell. In the limit of large supercells, the system studied corresponds to that of an isolated Zn_{In} impurity in the NWs.

The binding energies of the impurity states computed for different sizes of the supercells are shown in Figure 3 for the NWs with diameters 0.96 and 1.91 nm for both nondegenerate (up triangles) and doubly degenerate (down triangles) impurity levels. The binding energy of the triply

degenerate state (Figure 2a) computed from our theoretical approach in the bulk limit is also shown for comparison (0.034 eV, dashed line). The calculations for the thinnest NW studied, extended until convergence in the results was attained, determine the singly and doubly degenerate levels introduced by the isolated impurity to be located within the band gap of the NW, 0.198 and 0.052 eV above its VBM, respectively. The trend shown in the figure for the wider NW is well defined: the difference in the positions between singly and doubly degenerate states decreases with increasing diameter of the NW. The states eventually merge to form the bulk triply degenerate state. Our results show that the binding energies decrease as the separation between impurities decreases, indicating the tendency of impurities to bond. Also, the variation of the binding energies is less pronounced for the wider NW than for the narrower. This is consistent with the fact that the impurity states are less extended along the growth direction of the NWs in the wider NW.

The acceptor impurity state and the VBM state react similarly to confinement as they have similar character. The difference in their behavior as a function of confinement arise from the higher localization of the impurity state (Figure 2b) with respect to the extended VBM state (Figure 2d). The VBM is reduced in energy more rapidly than the impurity state as the diameter of the NWs decreases (the more localized a level is, the less it is affected by confinement). The binding energy of the acceptor state will increase monotonically with decreasing diameter (or increasing confinement) in the NW, having its maximum value at the thinner NW studied (~ 0.2 eV). The situation is different for the doubly degenerate state. In this case, the binding energy of the impurity state is determined by two compensating mechanisms due to confinement: the high localization of the state, which will try to move the extended VBM state to a lower energy with respect to the impurity state, and its radial character, which will produce the opposite effect. As a result, the doubly degenerate impurity state in the thinner NW takes almost the same position within the band gap as the impurity state in the bulk.

The predicted increase in the binding energy of the acceptor impurity state implies a limitation in the carrier concentration of holes in the NW. In the thinner NWs, only a small fraction of the impurities will ionize and contribute to free carriers. As such, the density of carriers is expected to be low. This result is a consequence of the effect of quantum confinement on the binding energy of the impurity state, that is, it is a result inherent to the p-type doped NW. Other factors limiting the density of free carriers in the NW could be the presence of native defects and the clustering of the Zn impurities to form precipitates, which are not considered here.

We also examined the effect of changing the location of the Zn within the wire. Initially, the Zn_{In} impurity was positioned within the NW so that two conditions were met: (1) the Zn was placed at the center of the NW, and (2) the T_d crystal symmetry of the NW in the vicinity of the impurity was preserved. This “bulk-like” placement of the impurity will be energetically favorable for the thick NWs constructed

experimentally (see Figure 1). We found the energy to be unfavorable if the impurity was displaced from the center of the NW toward the surface with the energy difference increasing with the diameter of the NW. We calculated the energy required to displace the Zn for the NWs with diameters 0.96, 1.43, and 1.91 nm to be 0.35, 0.43, and 0.48 eV, respectively.

Our results serve not only to characterize the acceptor impurity state introduced experimentally in Zn-doped InP-NWs, but also to predict the effects that the quantum confinement will have on this state. Figure 2b shows that the nondegenerate acceptor state is mainly distributed along the unconfined dimension of the NW. Therefore, we do not expect any qualitative differences in our results for this state when either one of the above two conditions is not satisfied. To justify this prediction, we performed a number of tests. In the first test, we placed the Zn_{In} impurity in the other two nonequivalent fourfold P-coordinated In sites of the 0.96 nm NW. These sites correspond to the sites occupied by each of the three fourfold-coordinated In atoms of parts b and c of Figure 2 located one and two layers away from the impurity. Displacing the impurity from the center of the NW results in the splitting of the 2-fold degenerate impurity levels, following the reduced symmetry of the impurity potential along the radial dimension of the NW. The total energy of the doped NW increases when the symmetry is reduced. In general, the total energy of the doped system is found to be determined by the radial coordinate of the Zn_{In} impurity, the energy increases with increasing displacement. In the second test, we relaxed the ionic positions of the first and second neighbor atoms surrounding the impurity atom placed at the central position. The atomic relaxation lowers the T_d symmetry of the impurity site to a trigonal C_{3v} symmetry through the deformation of the three Zn–P bonds in the radial dimension of the NW, with the subsequent lowering in energy of the twofold degenerate impurity state. In all these tests, the position of the singly degenerate acceptor state agrees to better than 0.02 eV with the values reported in Figure 3 for the same supercells.

In summary, we studied Zn-doped InP-NWs using first-principles calculations based on a real-space pseudopotential approach. The acceptor state introduced in the NWs is identified as a singly degenerate state with anion p character aligned along the growth direction of the NW. The binding energy of the state has been found to increase monotonically with decreasing diameter of the NW as a result of the two-dimensional confinement on the electronic states. A maximum binding energy of ~ 0.2 eV is predicted to be reached in the thinner NWs. The properties characterizing the acceptor impurity state are found to not depend significantly on the location of the Zn_{In} impurity within the host nanomaterial.

Acknowledgment. This work was funded by the Spanish Ministry of Education and Science (program “Ramón y Cajal” and project FIS2005–04239), by the U.S. National Science Foundation under DMR-0551195, and by the U.S. Department of Energy under DE-FG02-06ER46286 and DE-FG02-06ER15760. Computational support was provided by

the Barcelona Supercomputing Center (BSC), by the Galician Supercomputing Center (CESGA), by the Minnesota Supercomputing Institute, and by the Texas Advanced Computing Center (TACC).

References

- (1) Peercy, P. S. *Nature (London)* **2000**, 406, 1023.
- (2) Huang, Y.; Lieber, C. M. *Pure Appl. Chem.* **2004**, 76, 2051.
- (3) Yu, H.; Li, J.; Loomis, R. A.; Wang, L.-W.; Buhro, W. E. *Nat. Mater.* **2003**, 2, 517.
- (4) Gudiksen, M. S.; Wang, J.; Lieber, C. M. *J. Phys. Chem. B* **2002**, 106, 4036.
- (5) Duan, X. F.; Huang, Y.; Cui, Y.; Wang, J.; Lieber, C. M. *Nature (London)* **2001**, 409, 66.
- (6) See <http://www.ices.utexas.edu/parsec/>.
- (7) Alemany, M. M. G.; Jain, M.; Kronik, L.; Chelikowsky, J. R. *Phys. Rev. B* **2004**, 69, 075101; Alemany, M. M. G.; Jain, M.; Tiago, M. L.; Zhou, Y.; Saad, Y.; Chelikowsky, J. R. *Comp. Phys. Commun.* **2007**, accepted for publication.
- (8) Troullier, N.; Martins, J. L. *Phys. Rev. B* **1991**, 43, 1993.
- (9) Ceperley, D. M.; Alder, B. J. *Phys. Rev. Lett.* **1980**, 45, 566.
- (10) Huang, X.; Lindgren, E.; Chelikowsky, J. R. *Phys. Rev. B* **2005**, 71, 165328.
- (11) Gudiksen, M. S.; Wang, J.; Lieber, C. M. *J. Phys. Chem. B* **2002**, 105, 4062.
- (12) The value of the equilibrium lattice constant obtained from the ab initio pseudopotentials employed in this work, 5.85 Å, is in very good agreement with the value obtained from experiment, 5.87 Å.
- (13) Li, J.; Wang, L.-W. *Nano Lett.* **2004**, 4, 29; Li, J.; Wang, L.-W. *Chem. Mater.* **2004**, 16, 4012.
- (14) Bruno, M.; Palummo, M.; Marini, A.; Del Sole, R.; Olevano, V.; Kholod, A. N.; Ossicini, S. *Phys. Rev. B* **2005**, 72, 153310.
- (15) Schmidt, T. M.; Miwa, R. H.; Venezuela, P.; Fazzio, A. *Phys. Rev. B* **2005**, 72, 193404.
- (16) Hybertsen, M. S.; Louie, S. G. *Phys. Rev. B* **1986**, 34, 5390.
- (17) Zhao, X.; Wei, C. M.; Yang, L.; Chou, M. Y. *Phys. Rev. Lett.* **2004**, 92, 236805.
- (18) Mattila, T.; Zunger, A. *Phys. Rev. B* **1998**, 58, 1367.
- (19) Hirano, R.; Kanazawa, T.; Inoue, T. *J. Appl. Phys.* **1992**, 71, 659.
- (20) This finite-size fit expects the wave function of the impurity state to decay with an exponential tail. See Menchero, J. G.; Capaz, R. B.; Koiller, B.; Chacham, H. *Phys. Rev. B* **1999**, 59, 2722.

NL070344O